# 3. Prediction & Power Estimation

## *3.1 Predictive Filters & Power Estimation*

Generally, a prediction based on $N$ past signal samples and $M$ past predictor outputs is given [Orf90] by

$$\hat{y}(n+1) = \sum_{l=0}^{N-1} b(l)y(n-l) - \sum_{m=0}^{M-1} a(m)\hat{y}(n-m) \tag{3.1}$$

where $n$ is a discrete time sample index, $b(l)$ and $a(m)$ are predictor coefficients, $y(n)$ is a noisy predictor input signal sample, i.e., in this work, a received power level measurement or component of the received complex-valued baseband equivalent signal, and $\hat{y}(n)$ is the corresponding predictor output. The noiseless counterpart of the signal $y(n)$ is denoted later by $x(n)$.

As the baseband equivalent signal concerned is complex-valued, there are three possibilities for predictive power estimation. The predictive filtering can be done using real-coefficient predictors either to predict the components independently with two predictors Fig. 3.1(b), or to predict the signal power as such with a single predictor, Fig. 3.1(a) [Hua95]. It is also possible to use complex-coefficient predictors to predict the complex-valued baseband signal [Har95]. From the analysis point of view, it is sufficient to consider here only the real-coefficient cases. The extension to the complex-coefficient predictors can be done if desired.

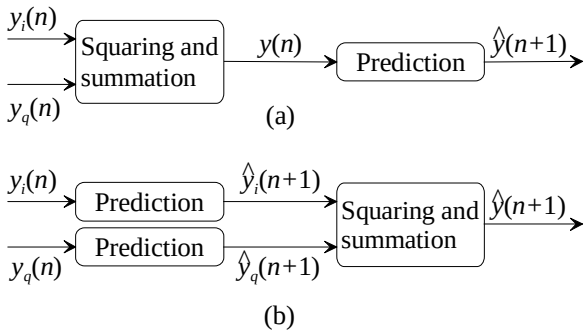


**Fig. 3.1.** Power prediction schemes for complex-valued signals. $y_i(n)$ and $y_q(n)$ are the noisy in-phase and quadrature components, respectively, $\hat{y}_i(n)$ and $\hat{y}_q(n)$ are the corresponding predictions, and $\hat{y}(n)$ is the prediction of the signal power.

### 3.1.1 Predictor Selection Criteria

In [P1] and [P2], the predictor selection criteria is the SNR gain achieved using H-N polynomial predictors with noisy, one-step-delayed Rayleigh distributed signals as inputs. The results are then used as reasonable choices for the predictors to be applied in the simulation setups in [P3] and [P4]. In this section, optimum H-N, and optimum power predictors for each mobile speed are found in a more consistent and unified manner. Two criteria, minimum mean squared error (MSE), and Minimum Description Length (MDL) criteria [Ris84], [The92], [Gao96], [Gao97] given by

$$\sigma^2 = \tfrac{1}{S}\sum_{n=1}^{S}\big(y(n)-x(n)\big)^2 \tag{3.2}$$

and

$$\mathrm{MDL}(N) = S\ln\sigma_N^2 + N\ln S\,, \tag{3.3}$$

respectively, are used for filter design parameter selection. In (3.2) and (3.3), $S = 2\ \mathrm{s}\cdot 9600\ \mathrm{samples/s}$ is the number of samples used in evaluating the criteria, $x(n)$ is the ideal predictor output signal sample, $y(n)$ the actual predictor output sample, and $N$ the length or order of the predictor. The subscript $N$ denotes that the quantity is calculated for the predictor of length or order $N$. MDL is actually a criteria used for finding the order of an autoregressive (AR) process [The92], and can also be used in determining the topology of neural networks [Gao96], [Gao97c]. As our Rayleigh fading process is not an AR process (cf. Section 4.3, Radio Channel Model), the MDL, or any other AR process order selecting criteria, cannot be expected to give exact results, and therefore it is always compared with the mean squared error criterion. The criteria are always evaluated using a different but statistically equivalent set of fading signal samples from that used in designing the predictors. Both criteria are evaluated over two seconds of Rayleigh fading channel power response for each noise level and mobile speed applied in the COSSAP simulations. The predictor design parameters over which the optimization is performed using MSE is given in [P5], except for the linear AR predictors which are shortly discussed in Section 3.1.4 below. The treatments in [P5] and in Section 3.1.4 are exactly analogous.

The Heinonen-Neuvo (H-N) and optimum predictors, reviewed below, are designed for the single user simulations for Rayleigh fading signal components with AWGN variances 0.1, 0.2, …, 0.9 for mobile speeds 10 km/h and 30 km/h, for 5 and 10 user simulations also for Rayleigh fading signal components but with AWGN variance 0.05, modeling receiver noise (and adjacent cell interference) and for mobile speeds 5 km/h, 10 km/h, …, 45 km/h, and finally, for the AWGN multiuser interference model simulations for fading signal components with AWGN variances of 1 and 5 for mobile speeds of 10 km/h and 30 km/h.

### 3.1.2 Heinonen-Neuvo Polynomial Predictors

As a class of finite impulse response (FIR) type predictors is considered in this work, the prediction (3.1) reduces to [Orf90]

$$\hat{y}(n+1) = \sum_{l=0}^{N-1} b(l)\,y(n-l)\,. \tag{3.4}$$

A filter of the form given in (3.4) is naturally inherently stable when $b(l)$ and $y(n)$ are bounded. With general infinite impulse response (IIR) predictors, given by (3.1), the stability would have to be separately proved in order to safely employ them in the closed power control loop. This is a natural requirement for the closed control loop to remain stable. To estimate a Rayleigh distributed signal by polynomials, the coefficients $b(l)$ are chosen to minimize noise gain when the predictor input signal is a low-degree polynomial corrupted by Gaussian noise. These predictors are generally know as Heinonen-Neuvo (H-N) polynomial predictors [Hei88], and have closed form predictor coefficients for given low degree of polynomial input signals. The coefficients $b(l)$ for the first and second degree predictors are given by

$$b_1(l) = \frac{4N - 6l + 2}{N(N-1)} \tag{3.7}$$

$$b_2(l) = \frac{9N^2 + (9 - 36l)N + 30l^2 - 18l + 6}{N^3 - 3N^2 + 2N} \tag{3.6}$$

where the subscript of *b* denotes the degree of the polynomial input signal for which the coefficients are optimized. From Fig. 3.2 it can be seen that the Rayleigh distributed signal piecewisely greatly resembles polynomials, and thus the approach is intuitively attractive. The Rayleigh fading prediction simulation results can also be interpreted as reflecting the amount of polynomial-like behavior of the Rayleigh fading signals. The Rayleigh signal in Fig. 3.2 is produced from the outputs of the noise shaping Rayleigh fader model in COSSAP, described later in Section 4.3.

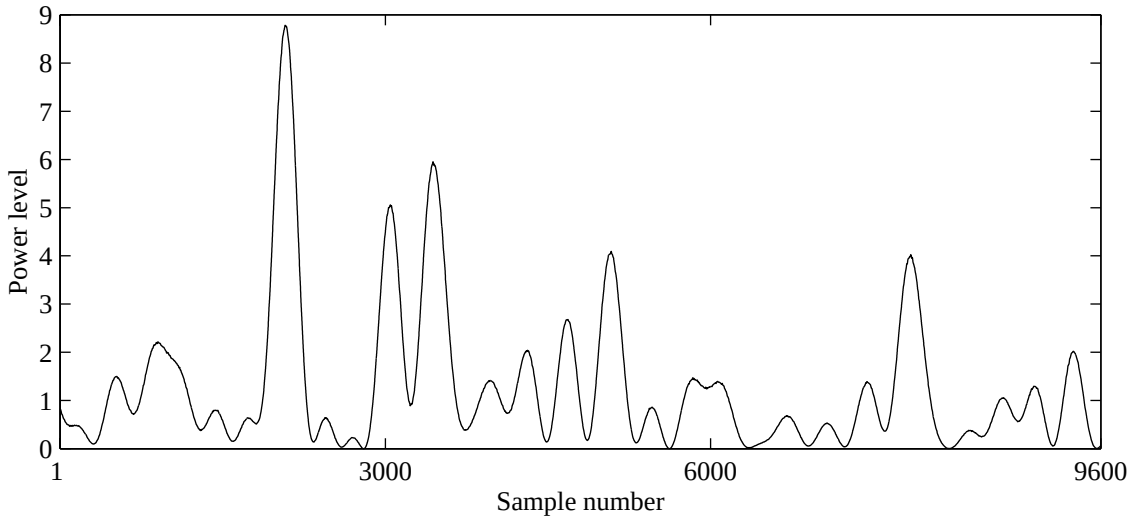


**Fig. 3.2.** One second of Rayleigh fading received signal power at the mobile speed of 10 km/h with the carrier frequency of 1.8 GHz.

To illustrate the prediction tools, some H-N predictor frequency and phase responses are shown in Figs. 3.3 through 3.6. The frequency responses of the first degree H-N predictors of lengths $N = 4, \ldots, 50$, and the group delays for the first degree, but lengths $N = 4, \ldots, 25$, within the frequency band of interest are more illustratively shown in Figs. 3.7 and 3.8, respectively. It is seen from Figs. 3.3, 3.5, and 3.7, that H-N predictors are lowpass filters with passband bandwidth decreasing with increasing filter length. As the polynomial degree is increased, the passband of the equally long predictors grows wider and also the passband peak increases. The prediction bandwidth, i.e., the frequency band within which the group delay is sufficiently close to -1, Figs. 3.4, 3.6 and 3.8, increases with the increasing polynomial degree. The prediction band in Figs. 3.4, 3.6 and 3.8 is actually seen to be quite narrow. This means that only the low frequency components of the Rayleigh fading signal power are actually predicted, the rest of the signal is more or less only filtered with a lowpass filter.

The MSEs and MDLs resulted of filtering a test Rayleigh fading signal component at 10 km/h, with added AWGN variance of 0.05, with H-N predictors of degrees $L = 1, 2$, and 3, and lengths $N = 4, \ldots, 50$, are shown in Figs. 3.9 and 3.10, respectively. The same results for mobile speed of 40 km/h are shown in Figs. 3.11 and 3.12, respectively. At 10 km/h, the

minima of MSE and MDL are found at first degree predictors of lengths $N = 40$ and $N = 39$, respectively, while at the higher speed of 40 km/h, Figs. 3.11, and 3.12, the optimum is reached at the filter degree two and length $N = 30$ for both MSE and MDL criteria. The sampling rate of the fading signal is 9600 Hz, and the carrier frequency 1.8 GHz.

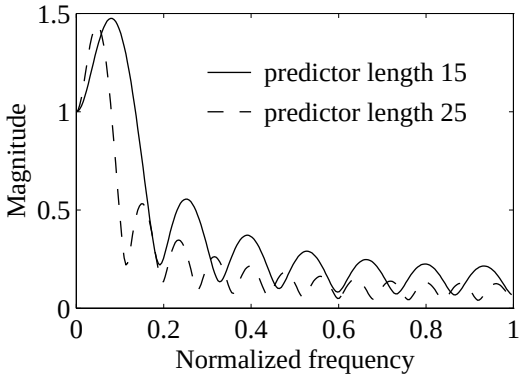


**Fig. 3.3.** Frequency responses of the 1st degree H-N predictors of lengths 15 and 25.

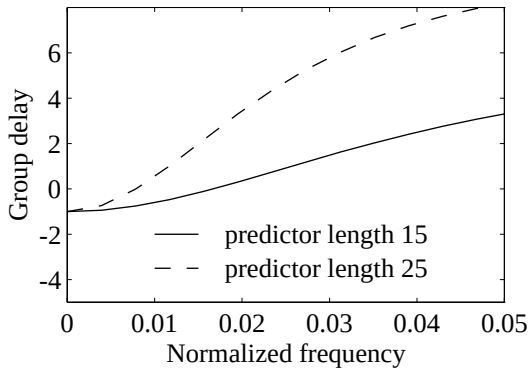


**Fig. 3.4.** Group delays of the 1st degree H-N predictors of lengths 15 and 25 (note the frequency scale).

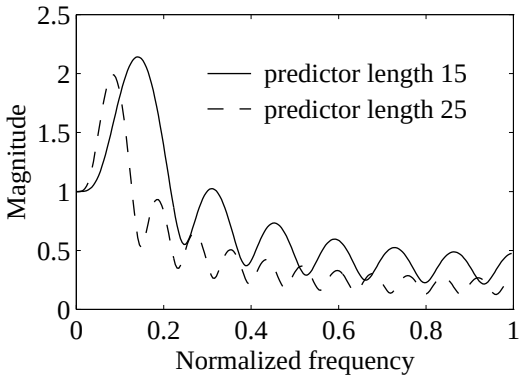


**Fig. 3.5.** Frequency responses of the 2nd degree H-N predictors of lengths 15 and 25.

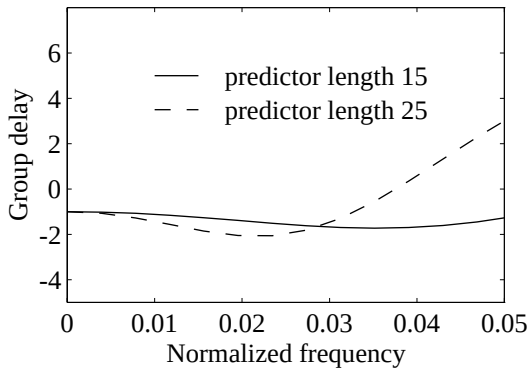


**Fig. 3.6.** Group delays of the 2nd degree H-N predictors of lengths 15 and 25 (note the frequency scale).

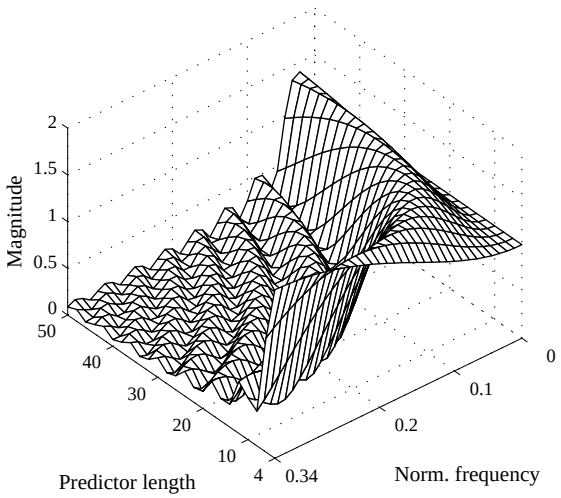


**Fig. 3.7.** Frequency responses of the 1st degree H-N predictors of lengths 4, ..., 50. Normalized frequency 0.34 is the maximum Doppler shift encountered in power signal at 50 km/h.

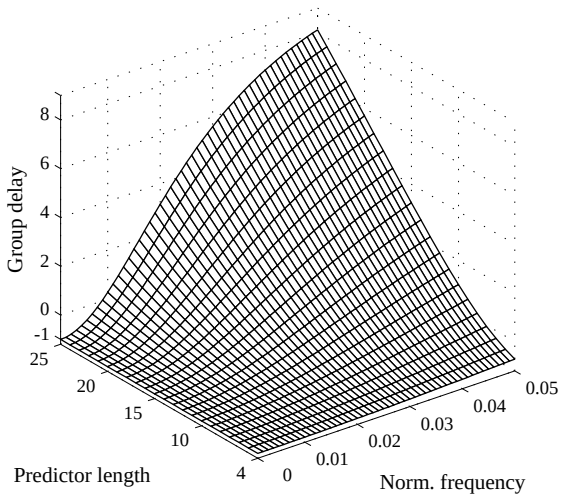


**Fig. 3.8.** Group delays of the 1st degree H-N predictors of lengths 4, ..., 25 (note the scales).

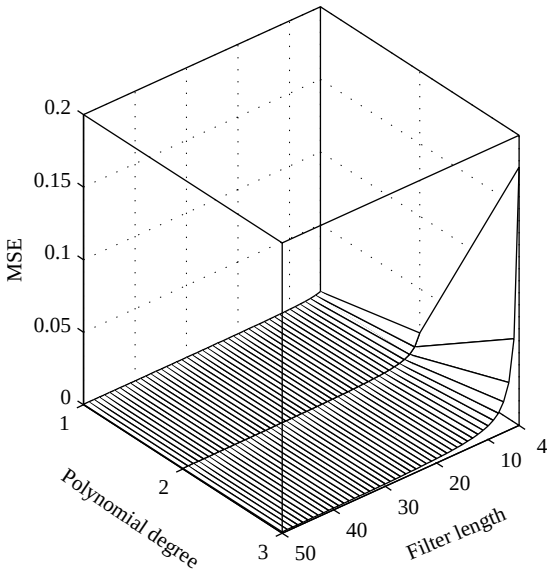


**Fig. 3.9.** MSE error surface for H-N predictors filtering the in-phase component of Rayleigh fading at 10 km/h with component AWGN variance 0.05.

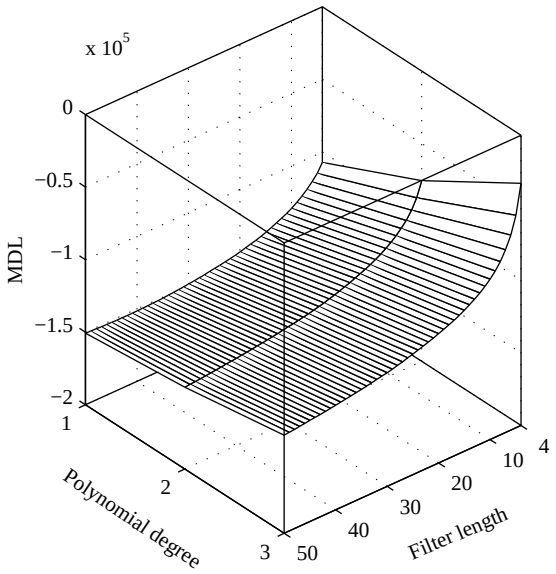


**Fig. 3.10.** MDL surface for H-N predictors filtering the in-phase component of Rayleigh fading at 10 km/h with component AWGN variance 0.05.

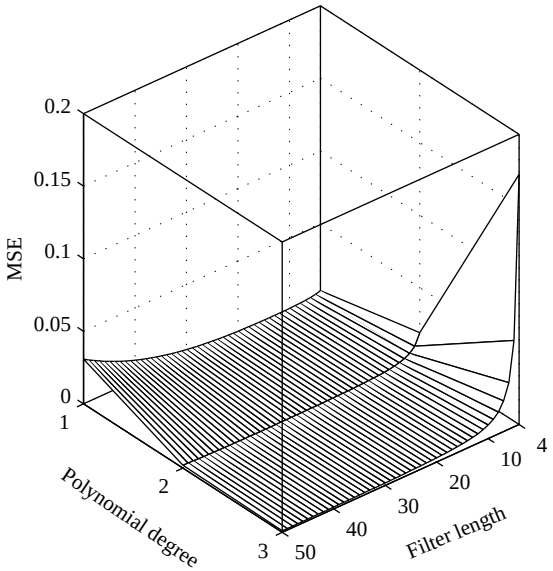


**Fig. 3.11.** MSE error surface for H-N predictors filtering the in-phase component of Rayleigh fading at 40 km/h with component AWGN variance 0.05.

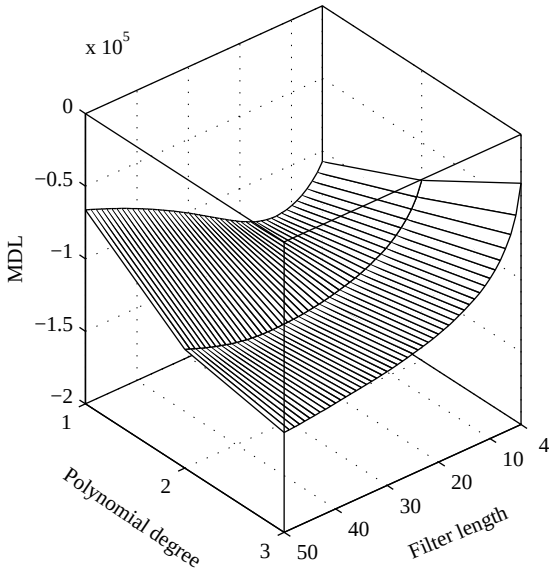


**Fig. 3.12.** MDL surface for H-N predictors filtering the in-phase component of Rayleigh fading at 40 km/h with component AWGN variance 0.05.

For further reading on predictive filtering, please, refer to publications of Ovaska [Ova], Laakso [Laa] and Ranta [Ran].

### 3.1.3 Optimal Power Estimators

Optimal power estimators based on both Hammerstein model (HM) and Wiener model (WM) are developed by A. Huang, and described and simulated in [Hua95a], [Hua95b], [Hua96a],

[Hua96b], [Hua96c], [Hua97] which is her Licentiate Thesis and a counterpart to this Thesis, [Hua98], and [P5].

General quadratic filtering (QF) [Pic82], [Sic92], [Fan95] is not well suited for practical real time application because of massive computations needed. Two simple structures [Fan95] of QF, HM and WM, with low computational requirements are of interests, though. Huang (see references above) has analyzed these models for complex-valued signals. A power estimator for complex-valued signals based on HM is illustrated in Fig. 3.1(a), and a WM based estimator in Fig. 3.1(b).

In WM based estimators, a global optimization yields a solution which is only applicable as numerical solutions for filter coefficients though iterative calculations. On the other hand, the estimator, Fig. 3.1(b) can be partially-optimized in closed form by solving for optimal estimation at the output of the filters, i.e., the overall power estimator is partially-optimized. For the results and derivations on optimum power estimators based on WM, please refer to [P5], or to [Hua98] in which the filter design more elaborately presented. Results in [P5] are achieved employing partially-optimized power estimators based on WM. HM based power estimator were not employed in the simulations presented in *the Publications*.

The predictor parameter selection method employed is described in [P5] with notes on the applicability to the power control problem at hand. Frequency responses and group delays of three of the resulted optimum predictors based on WM are shown in Figs. 3.13 and 3.14, respectively. The design parameters for the predictors, in Figs. 3.13 and 3.14 are selected according to the minimum MSE criterion. The minimum MSEs are found at predictor length $N = 50$ designed using 13200 prototype signal samples for 10 km/h case, at $N = 50$ designed with 15000 samples for 30 km/h, both with component AWGN variance of 0.05, and for 30 km/h with high component noise variance of 5, at length $N = 50$, designed using 2400 prototype signal samples. The optimum predictor designed for 30 km/h and noise variance of 0.05 possesses an actual prediction band, Fig. 3.14. The minimum MSE and MDL for 10 km/h, in Figs. 3.15 and 3.16, are both found with filter length 50 designed using 13200 prototype signal samples, while for 40 km/h, Figs. 3.17 and 3.17, the minimum is at filter length 24, designed using 15000 prototype signal samples for both criteria.

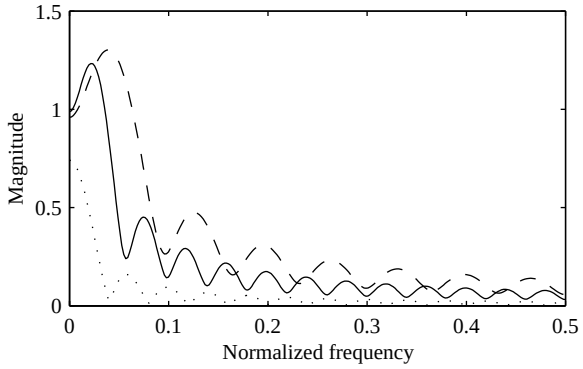


**Fig. 3.13.** Frequency responses of the optimum predictors designed for 10 km/h (solid) and 30 km/h (dashed) with component noise variance 0.05, and for 10 km/h and noise variance of 5 in components (dotted) (note that the frequency scale is up to half the Nyquist rate).

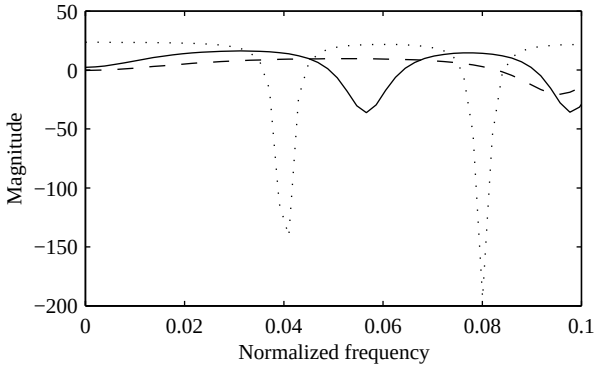


**Fig. 3.14.** Group delays s of the optimum predictors designed for 10 km/h (solid) and 30 km/h (dashed) with component noise variance 0.05, and for 10 km/h and noise variance of 5 in components (dotted) (note the frequency scale).

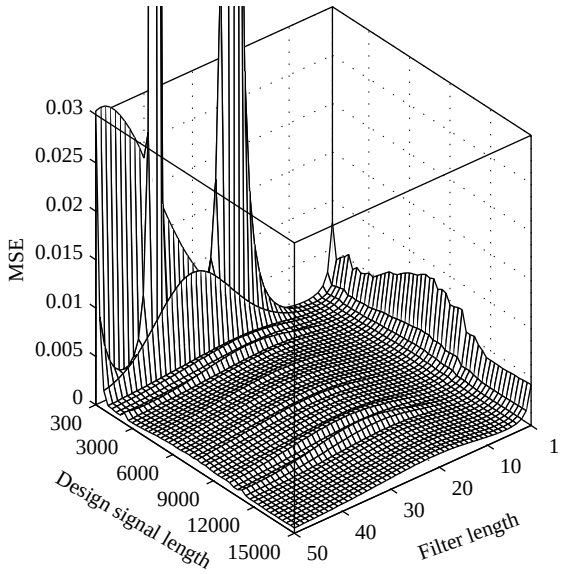


**Fig. 3.15.** MSE error surface for optimum predictors designed and tested with the in-phase component of the Rayleigh fading at 10 km/h with component AWGN variance 0.05.

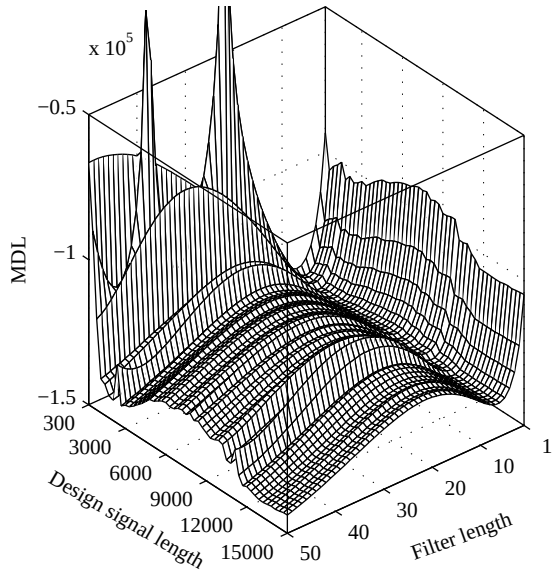


**Fig. 3.16.** MDL surface for optimum predictors designed and tested with the in-phase component of the Rayleigh fading at 10 km/h with component AWGN variance 0.05.

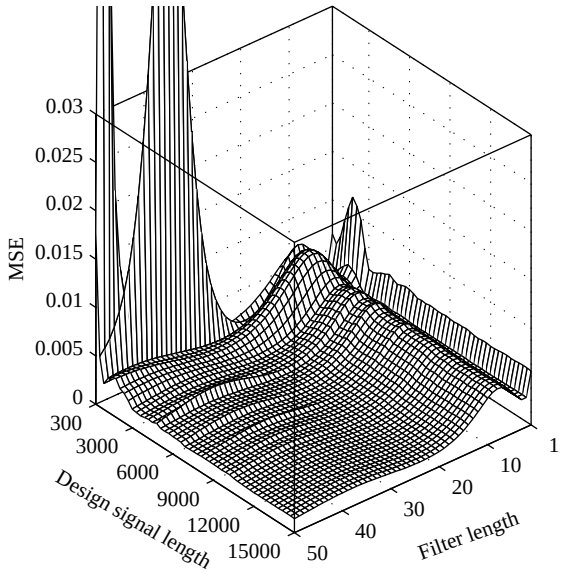


**Fig. 3.17.** MSE error surface for optimum predictors designed and tested with the in-phase component of the Rayleigh fading at 40 km/h with component AWGN variance 0.05.

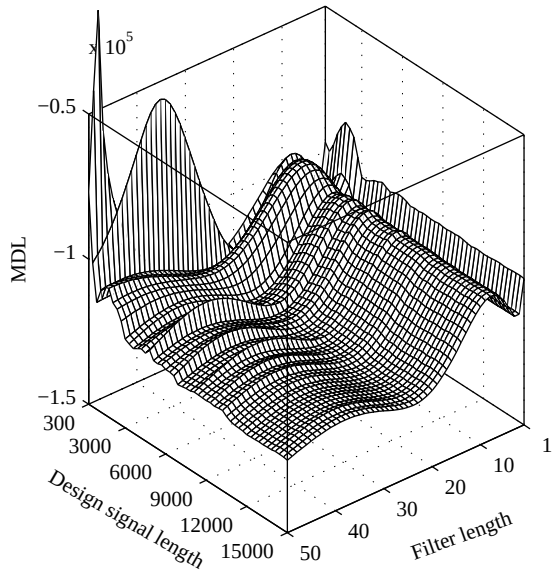


**Fig. 3.18.** MDL surface for optimum predictors designed and tested with the in-phase component of the Rayleigh fading at 40 km/h with component AWGN variance 0.05.

The fact that the filter coefficient optimization is performed for a predefined predictor length, results in that the prediction quality is to a large extend not dependent on the predictor length. This is seen as the large flat near-minimum MSE, and MDL, regions in Figs. 3.15 and 3.16, respectively. This property is less pronounced in the high speed case, illustrated by the MSE and MDL surfaces in Fig. 3.17 and 3.18, respectively. The nearly flat close-to-minimum regions in the MSE and MDL figures, Figs. 3.15, …, 3.18, actually mean that it is not necessary to perform strict optimization of the filters lengths and prototype signal lengths but little. This fact is employed in [P5] by designing optimum predictors with ad hoc selected

design parameters; length $N$=15, designed using 3000 prototype signal samples, i.e., predictors within the flat region, for each mobile speed and noise level. These predictors are then applied in all the same simulations presented for the optimum optimized predictors in [P5].

The results in [P5] confirm the above statement about the freedom to set the filter length and filter design prototype signal length. In [P5], it is seen that the simulation results do not greatly depend on whether the design parameters are optimized or selected ad hoc from the flat nearly-optimal design parameter region.

### 3.1.4 Linear Predictors

Originally intended as reference predictors for the research in this Thesis, also linear AR predictors are designed. Here the difficulty arises from the order selection [The92] of the predictor since in practice the actual order of the fading process would next to impossible to know accurately. In the simulations, the fading process is naturally known. The linear AR predictors are designed using the autocorrelation method [The92] with exactly the same filter design prototype signals as used for the optimum predictor design. The parameter selection method used in exactly analogous to that described in [P5] in Section II C.

MSE and MDL surfaces for 10 km/h and AWGN variance of 0.05 are plotted in Figs. 3.19 and 3.20, respectively. The minimum MSE is found at filter length $N$ = 15, designed using 300 prototype signal samples, while MDL criterion yields the predictor of length one, designed also using only 300 prototype signal samples.

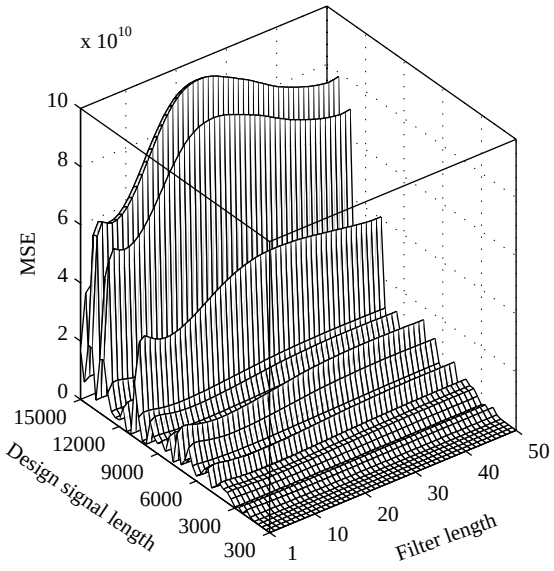


**Fig. 3.19.** MSE error surface for linear AR predictors designed and tested with the in-phase component of the Rayleigh fading at 10 km/h with component AWGN variance 0.05.

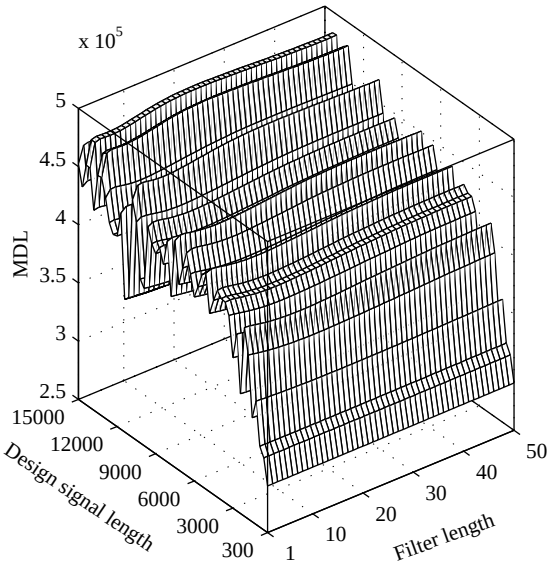


**Fig. 3.20.** MDL surface for linear AR predictors designed and tested with the in-phase component of the Rayleigh fading at 10 km/h with component AWGN variance 0.05.

The high MSE levels reveal that these predictors are not applicable to the problem at hand. Their frequency responses look actually worse than what could be considered decent to be shown here.

### 3.1.5 LS Optimal Predictors

Least squares (LS) optimal predictors [Kal85] are used as upper bounds for the performance evaluations with Rayleigh fading predictive filtering using H-N predictors in [P1] and [P2], in which also the applied LS predictor design principles are given.